TRANSIENT BASED EARTH FAULT LOCATION IN 110 KV SUBTRANSMISSION NETWORKS

Peter Imriš
Researcher
Helsinki University of Technology, Finland
Peter.Imris@hut.fi

Matti Lehtonen
Professor
Helsinki University of Technology, Finland
Matti.Lehtonen@hut.fi

1 ABSTRACT

This paper presents the analysis of ground fault transients in high voltage networks for fault location purposes. The practical application of the charge transient in 110 kV networks using of low frequency records is the main subject of this paper. Two algorithms for the fault computation, the wavelet and the differential equation method, are presented and compared. The paper also tries to point out the main sources of error affecting the method accuracy.

Keywords: differential equation algorithm, fault location, single-phase to ground faults, 110 kV overhead lines, wavelet algorithm, wavelet filter.

2 INTRODUCTION

Ground fault signals consist of different frequency components, which result from charging or discharging of the network capacitances. The charge transient is generated by the voltage rise in sound phases during a single-phase to ground fault. This means that a charge transient is always a side effect of the ground fault. Moreover, it is typically of strong amplitude and therefore is reasonable to use for single-phase to ground fault location. The practical application of the charge transient in 110 kV networks is the main subject of this paper.

Previous research on this topic can be found in [1]-[5], mainly for MV level networks. The testing of fault transients for fault location with the EMTP/ATP software can be found in [7].

All data used in the paper were recorded in a 110 kV Finnish network. The recorded data are processed by the Matlab. Basically, the fault's signal processing has two stages. First, the pre-processing takes place, the main task of which is to prepare the measured signals and then the fault location method is applied. The fault location algorithm applied to the fault signals is the main processing methods, [1] - [3].

For improving the method for future applications, it is also important to study the sources of error affecting the method accuracy.

3 SIGNAL PRE-PROCESSING

The fault transients are mixed with the other signals as noise and fundamental frequency component. Sometimes the transient can be short in time and also small in amplitude, moreover it can be very close to the fundamental frequency signal in the frequency domain. Therefore, the 50 Hz component can negatively affect the fault transient frequency estimation. To enable a more precise analysis of the fault transient, pre-processing is performed. It contains:

1. Digital band-pass FIR filter.
2. Charge transient frequency detection.
3. Wavelet filter.

The digital FIR filter main purpose is to remove the 50 Hz signal, its lower frequency is set on $v_{c1} = 100Hz$ and higher set on $v_{c2} = 500Hz$, as in the Fig. 1, where the filter's frequency response is shown.

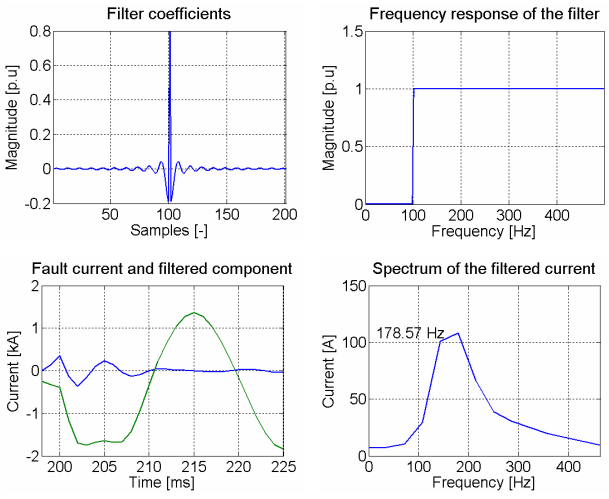

Fig. 1 Pre-processing of the fault signals, (case: 01.09 2002).

This filter characteristic can be achieved with the coefficients Eq. (1), given by the *sinc* function, [8].

$$h(k)=\frac{\sin(2\pi v_{c2}(k-l)}{\pi(k-l)}-\frac{\sin(2\pi v_{c1}(k-l)}{\pi(k-l)}\text{, if } k\neq l$$
$$h(k)=2(v_{c2}-v_{c1})\text{, if } k=l \qquad (1)$$

In order to reduce the pass-band and stop-band ripple we used the Hamming window, Eq. (2), as presented in [8]. The filter coefficients can be seen in Fig. 1.

$$w(k)=0.54-0.46\cos(2\pi k/(N-1)) \qquad (2)$$

Where k and l are the integer variables, N is the number of coefficients.

The example of filtered charge transient out of the fault current is shown in Fig. 1. After removing the 50 Hz the charge transient frequency is detected. The charge transient frequency is detected as a dominant frequency component of the filtered signal spectrum (in this case: 178.57 Hz, Fig. 1). The spectrum is calculated with a Fourier transform, [6].

The filtering of the signal is performed, in order to get the fault transient precisely out of the measured signal. Our filter is based on the wavelet. The wavelet filter is set exactly on the frequency of the measured (charge) fault transient estimated by the Fourier transform. The filters coefficient and its frequency response with an example fault current are shown in Fig. 2. The filter coefficients, in this case, are represented by a "Gaussian mother wavelet". More about the wavelet applied to the power system can be found in [6] and the practical implementation to the simulated ground fault transient in [7].

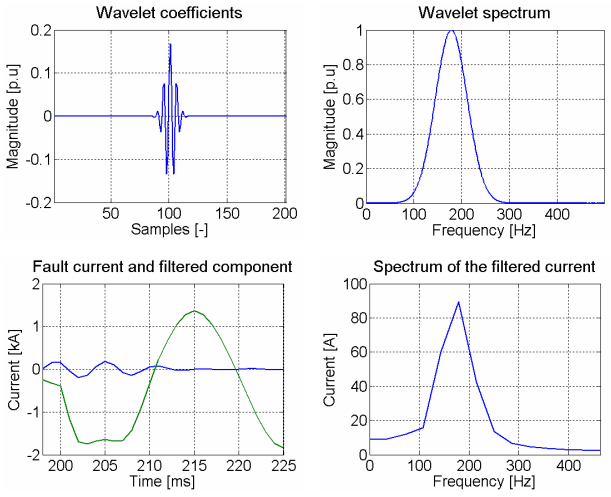

Fig. 2 Wavelet filter, (case: 01.09 2002).

The discrete wavelet transform is defined as:

$$DWT(a,b)=\frac{1}{\sqrt{|a|}}\sum_n x[n]\cdot\psi\left(\frac{n-b}{a}\right) \qquad (3)$$

Where: $x[n]$ is a discrete function of the samples, a is the scale, b is the translation, ψ is the mother wavelet, and $k, n,$ and m are integer variable parameters, with n in this case representing discrete time.

4 FAULT LOCATION ALGORIHMS

When an earth fault occurs, the voltage of the faulty phase falls and the charge stored in its earth capacitances is removed. This initiates the discharge transient. Because of the voltage rise of the two sound phases, another component, called the charge transient, is created, [2]. The charge transient is usually of higher amplitude and lower frequency than the discharge transient, which is more suitable for the purpose at hand. These transients can be used for fault location if they are detected. Transient fault location is based on the estimation of the fault path inductance L_f from the detected fault transients.

In this paper we consider the first order model of the line. This kind of line model takes into consideration only the resistance and inductance of the line. Any capacitances are not included in tested fault location equations.

The fault path inductance can be calculated directly from the filtered signal (the charge transient), using of so-called wavelet algorithm or a differential equation algorithm:

The equation for the wavelet algorithm, [2]:

$$L_f=\frac{1}{\omega_c}Im\left[\frac{v_c(t,f)}{i_c(t,f)}\right]=\frac{1}{3}(L_0+L_1+L_2)\cdot l_f \qquad (4)$$

Where ω_c, v_c and i_c are the angular frequency, voltage and current of the charge transient. The fault distance is l_f. L_0, L_1 and L_2 are the zero-, positive- and negative-sequence inductances of the faulty line per *km*. t represents time and f the frequency.

The equation for the differential equation algorithm, [1]:

$$L_f=\frac{\Delta t}{2}\left[\frac{(i_{k+1}+i_k)(v_{k+2}+v_{k+1})-(i_{k+2}+i_{k+1})(v_{k+1}+v_k)}{(i_{k+1}+i_k)(i_{k+2}-i_{k+1})-(i_{k+2}+i_{k+1})(i_{k+1}-i_k)}\right] \qquad (5)$$

Where Δt is a sampling time, v and i are the samples of faulty voltage and current, L_f is the inductance. The k is an integer variable.

5 ANALYSIS OF RECORDED GROUND FAULTS

All data used in the paper were recorded in the Finnish electricity transmission system operator's grid (110 kV), Fingrid Oyj, Finland. The sampling frequency is 1 kHz. All together, 6 cases were processed. All faults

were not permanent, therefore the exact position of the faults were calculated by the travelling wave fault locator connected in parallel to the transient recorder. Fault happens in the branch Pyhäkoski - Rautaruukki, Fig. 3.

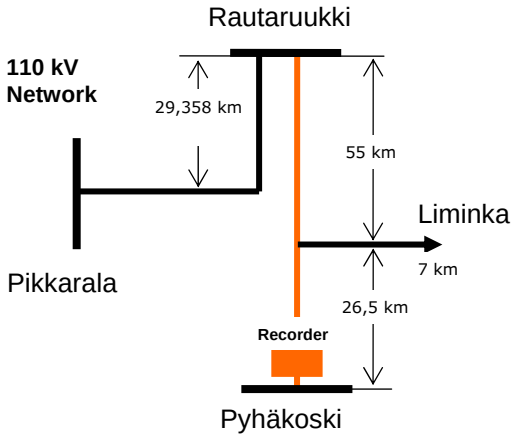

Fig. 3 The scheme of the network.

The line parameters for the studied network were calculated by the Carson's method [11], at frequency 150 Hz, ground resistivity $\rho = 3000\,\Omega m$ with the 500 iterations. The results are shown in Table 1.

Table 1 Symmetrical components of the line.

	Zero-sequence	Positive-sequence	Negative-sequence
L [mH/km]	2.5995	1.282	1.282
R [Ω/km]	0.19072	0.084854	0.084854

The analysis of these cases shows, that the differential equation algorithm is less dependent on the estimation of the transient frequency (frequency variation for all cases is in range 100-200 Hz). It is because the transient frequency does not directly exist in the fault location equation as in wavelet algorithm, compare Eq. (4) and Eq. (5). The results are shown in the following Table 2.

Table 2 Calculated fault distances of single-phase to ground faults.

Date of fault	Exact Fault distance [km]	Wavelet algorithm		Differential equation algorithm	
		Fault distance [km]	Error [km]	Fault distance [km]	Error [km]
30.06.2002	59	45,65	13,35	61	-2
27.07.2002	1	0,21	0,79	0,45	0,55
01.09.2002	25,8	25,92	-0,120	26,1	0,3
04.10.2002	73,3	82,73	-9,43	85	-11,7
19.05.2003	51,5	51,79	-0,29	52	-0,5
22.05.2003	51,5	50,48	1,02	50	1,5

The results of both algorithms are comparable. The error is primarily caused by the model simplicity (skipping the capacitances of the network) and the fault location equation is build for a radially operated system and our records are from system supplied from both ends. However, the results are relatively good.

Secondly, the error is also caused by the line parameters changing. Studying the line properties at different frequencies shows that the zero-sequence inductance of the line is dependent on the frequency. For the studied case of 100-200 Hz, the variation is approximately 0.86%. The positive sequence inductance is stable in this range. Changing of ground resistivity along the line might also affect.

The typical measurement transformers (CT and PT) of this voltage level measure such transients with accuracy as for 50 Hz, [9], [10].

However, the recorder sampling frequency is also low. In a case where the transients are damped very quickly the higher frequency is needed. Longer lasting transients do not require a higher sampling rate. In our case, increasing the sampling frequency to 5 kHz would improve the results significantly.

6 EXAMPLE

For better illustration of the algorithms application to the measured signal this example is shown. The fault event is recorded 1.9 2002, Table 2. The fault distance measured by travelling wave recorder was 25.8 km. The fault type is single-phase to ground. The fault voltages and currents (of all phases) can be seen in the following Fig. 4.

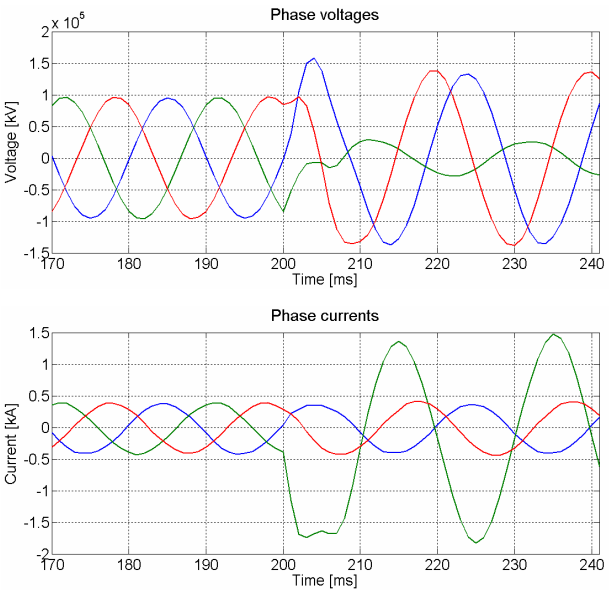

Fig. 4 The recorded single phase to ground fault: Phase voltages and currents, (case: 01.09 2002).

The pictures related to the pre-processing of charge transients in this case are shown in Fig. 1 and Fig. 2. The charge transient is of small amplitude and relatively low frequency as it can be seen in this specific case. The simulated charge transients in [7] by EMTP/ATP shows higher values (260-270 Hz). However, this value de-

pends too much on the transformer inductance. In this case the frequency is 178.57 Hz, Fig. 1.

The wavelet algorithm with using of Eq. (4) gives the result as in Fig. 5. Hence, the exact fault distance is taken as the stable part of the fault distance curve, while the transient exists.

The results of differential equation algorithm applied to the example signals is shown in Fig. 6. As it can be seen the stable part of the curve is indicating the fault distance.

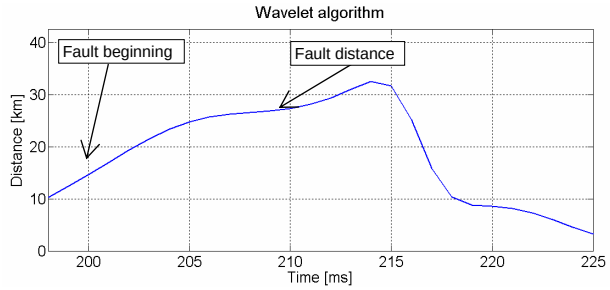

Fig. 5 Fault distance curve for the wavelet algorithm, (case: 01.09 2002).

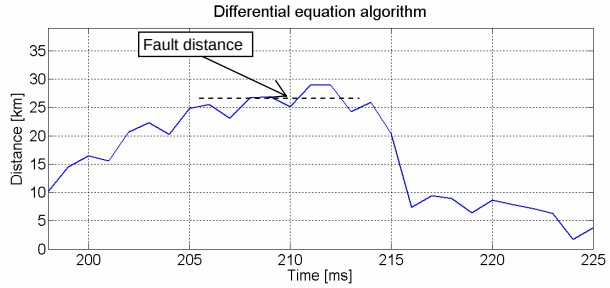

Fig. 6 Fault distance curve for the differential equation algorithm, (case: 01.09 2002).

7 CONCLUSIONS

The paper shows that single-phase to ground fault location using a charge transient is possible even if the sampling frequency of the records is only 1 kHz. Both the tested algorithms, the wavelet and the differential equation algorithms, behave similarly. The differential equation algorithm is less dependent on fault transient frequency estimation than the wavelet algorithm. The main result of this study is that both studied algorithms can be applied to the Finnish 110 kV subs-transmission lines with the present configuration. Better results will be expected when the sampling frequency is higher, preferably 5 kHz (or higher).

8 ACKNOWLEDGEMENT

This work was supported by Fingrid, to which the authors wish to express their warmest thanks.

REFERENCES

[1] Lehtonen, Matti. "Transient analysis for ground fault distance estimation in electrical distribution networks", Espoo 1992, Technical Research Centre of Finland, VTT Publications 115. 182p+app. 92p

[2] Hänninen, Seppo. "Single phase earth faults in high impedance grounded networks. Characteristic, indication and location". Espoo 2001. Technical Research centre of Finland, VTT Publication 453. 78p.+app.61p.

[3] Schegner, P.: Digitaler "Erdschlußuniversalschutz. Konzept und erste Realisierung". Dissertation, Universität des Saarlandes, Saarbrücken, 1989, 186 pp.

[4] Igel, M.: "Neuartige Verfahren für den Erdschlußdistanzschutz in isoliert und kompensiert betriebenen Netzen. Signale und Algoritmen im Frequenzbereich". Dissertation, Universität des Saarlandes, Saarbrücken, 1990, 181 pp.

[5] Pundt, H.: "Untersuchungen der Ausgleichsvorgänge bei Erdschluß in Hochspannungsnetzen mit isoliertem Sternpunkt und induktiver Sternpunkterdung als Grundlage zur selektiven Erdschlußerfassung". Dissertation, TU Dresden, 1963, 167 pp. + app.

[6] Robertson, D.C.; Camps, O.I.; Mayer, J.S.; Gish, W.B.; "Wavelets and electromagnetic power system transients", IEEE Transactions on Power Delivery, Volume: 11 , Issue: 2 , April 1996, Pages:1050 – 1058.

[7] Imriš, P.; Lehtonen, M.; "Transient based Ground Fault Location using Wavelets", The 4th IASTED International Conference on POWER AND ENERGY SYSTEMS, Rhodes, Greece, June 28-30, 2004, pp. 507-511.

[8] Stearns Samuel D., Digital Signal Processing with examples in Matlab, CRC Press LLC, 2000 N.W. Corporate Blvd., Boca Raton, Florida 33431., pp. 112-124

[9] Seljeseth, H.; Saethre, E.A.; Ohnstad, T.; Lien, I.;" Voltage transformer frequency response. Measuring harmonics in Norwegian 300 kV and 132 kV power systems", 8th International Conference on Harmonics And Quality of Power, 1998. Proceedings., Volume: 2 , 14-16 Oct. 1998, Pages:820 - 824 vol.2.

[10] Samesima, M.I.; de Oliveira, J.C.; Dias, E.M.; "Frequency response analysis and modeling of measurement transformers under distorted current and voltage supply", IEEE Transactions on Power Delivery, Volume: 6 , Issue: 4 , Oct. 1991, Pages:1762 – 1768.

[11] Carson, J.R., Wave propagation in overhead wires with ground return. Bell System Technical Journal, Vol. 5, 1926. pp. 539-54.